

# A Computational NMR Study of Boron Phosphide Nanotubes

Mahmoud Mirzaei

Young Researchers Club, Islamic Azad University, Shahr-e-Rey Branch, Shahr-e-Rey, Iran

Reprint requests to M. M.; E-mail: mdmirzaei@yahoo.com

Z. Naturforsch. **65a**, 844–848 (2010); received February 16, 2009 / revised January 20, 2010

Structural properties of two representative (4,4) armchair and (6,0) zigzag boron phosphide nanotubes (BP-NTs) are studied by density functional theory (DFT) calculations. To this aim, both structures and also the equivalent layer-like structures are individually optimized; afterwards, the boron-11 and phosphorous-31 chemical shielding (CS) tensors are calculated in the optimized structures. The calculated energies indicate that tubular structures are stabilized and the CS tensors are divided into some layers based on equality of electronic properties in the structures. All computations are performed by Gaussian 98 program package.

*Key words:* Boron Phosphide; Nanotube; Density Functional Theory; Chemical Shielding.

## 1. Introduction

Since carbon nanotubes (CNTs) [1] are metal or semiconductor depending on their tubular diameter and chirality, considerable efforts have been stimulated to synthesize non-carbon nanotubes with properties independent of the restricting factors [2–5]. The binary compounds of groups III and V are always semiconductors and suggested as proper alternative materials for the CNTs [6–9]. Among these materials, the tubular structure properties of the group III-nitrides, e. g., boron nitride (BN), aluminum nitride (AlN), gallium nitride (GaN), and indium nitride (InN) are more studied [10–13] than those of the group III-phosphides, e. g., boron phosphide (BP), aluminum phosphide (AlP), gallium phosphide (GaP), and indium phosphide (InP) [14]. Since the electronic properties of BP are similar to those of silicon carbide (SiC), much more attentions have recently been focused on the determination and characterization of the latter materials, the group III-phosphides [15–16]. Although the possibility of tubular structure of BP has not been examined up to now, but pioneering computational works can reveal new trends about the structural properties of this material for other researchers interested in this field. In present work, the structural stabilities of BP nanotubes (BP-NTs) are examined by performing density functional theory (DFT) calculations on the representative (4,4) armchair and (6,0) zigzag models (Fig. 1). The atomic geometries are allowed to relax by optimization, and the stabilization ener-

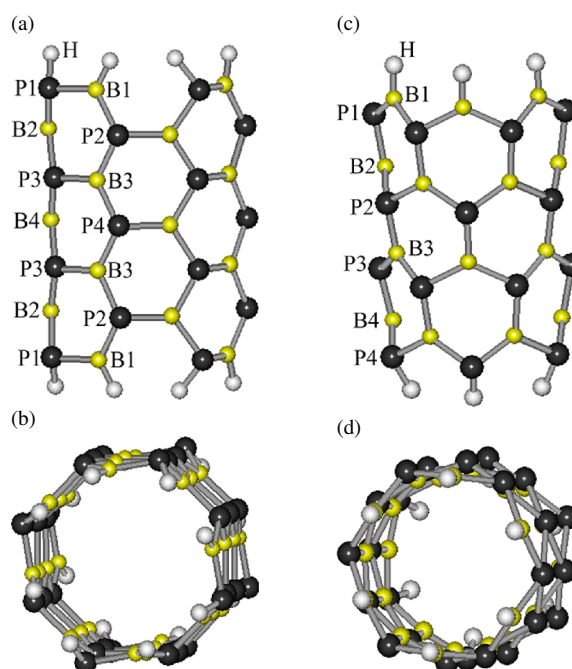


Fig. 1 (colour online). 2D views (a), (c) and 3D views (b), (d) of the (4,4) armchair (a), (b) and the (6,0) zigzag (c), (d) BP-NTs.

gies are calculated (Table 1). For a systematic investigation, the layer-like structures with the same numbers of atoms referring to the NTs are also considered in the calculations. Furthermore, chemical shielding (CS) parameters are also calculated for the stabilized structures of the considered NT and layer-like models

Table 1. Structural properties of BP-NTs and BP-layers.

Properties	(4,4)		(6,0)	
	NT	Layer-like structure	NT	Layer-like structure
Averaged B-P Length (Å)	1.89	1.87	1.90	1.88
Band Gap Energy (eV) <sup>a</sup>	2.95	1.08	2.27	1.68
Stabilization Energy (au)	-10264.04	-10263.72	-8796.71	-8796.54
Binding Energy (kcal/mol) <sup>b</sup>		-201.12		-106.80

<sup>a</sup> The energy difference between HOMO and LUMO. <sup>b</sup> The energy difference between NT and layer-like structures.

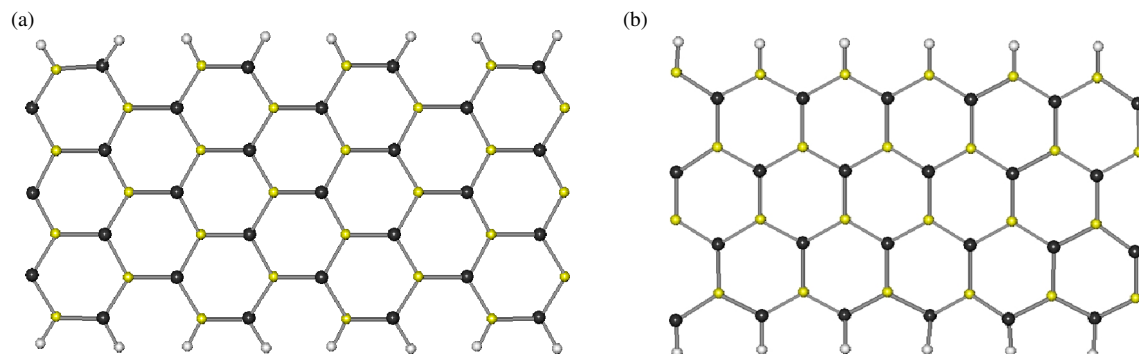


Fig. 2 (colour online). 2D views of the corresponding layer-like structures. The armchair ends of the corresponding (4,4) armchair structure (a) are saturated by the H atoms whereas the zigzag ends are left unsaturated. The zigzag ends of the corresponding (6,0) zigzag structure (b) are saturated by the H atoms whereas the armchair ends are left unsaturated.

(Tables 2 and 3). It is noted that nuclear magnetic resonance (NMR) spectroscopy is an insightful technique to study the structural properties of matters [17] and also the NTs [18–20].

## 2. Computational Details

Two representative armchair and zigzag models of the single-walled BP-NTs are considered within this work. The considered armchair model is a 12-Å length (4,4) BP-NT consisting of 28 B and 28 P atoms which 16 H atoms saturate the two ends of the tube (Fig. 1a, b). The considered zigzag model is a 12-Å length (6,0) BP-NT consisting of 24 B and 24 P atoms which 12 H atoms saturate the two ends of the nanotube (Fig. 1c, d). To compare the properties of tubular and layer-like structures, the corresponding finite sized layer-like models of the considered (4,4) and (6,0) NTs with the same numbers of atoms referring to the armchair and zigzag NTs are also considered. It is known that the layer-like structures have two zigzag and armchair ends, where binding of the zigzag ends due to rolling makes armchair NT, whereas binding of the armchair ends due to rolling makes zigzag NT. Therefore, in the corresponding layer-like structure of the (4,4) BP-NT, which consists of 28 B and 28 P atoms, the armchair ends are saturated by 16 H atoms but the zigzag

ends are left unsaturated (Fig. 2a). In the corresponding layer-like structure of the (6,0) BP-NT, which consists of 24 B and 24 P atoms, the zigzag ends are saturated by 12 H atoms but the armchair ends are left unsaturated (Fig. 2b). The structures are individually optimized employing B3LYP exchange-functional and 6-31G\* standard basis set by Gaussian 98 program package [21]. Afterwards, the <sup>11</sup>B and <sup>31</sup>P CS parameters are calculated for the optimized structures at the same level of theory based on the gauge included atomic orbital (GIAO) approach [22]. Local gauge origin was initially suggested by London [23] for study of the molecular diamagnetism to define the vector potential of the external magnetic field. Ditchfield [24] then adapted the idea in the GIAO method for magnetic shielding calculations. According to the work of Ditchfield, in which each atomic orbital has its own local gauge origin placed on its center, Prado et al. [25] and Fukui et al. [26] implemented the GIAO method. CS is a local property belonging to each nucleus depending on the external magnetic field. The isotropic CS ( $\sigma_{\text{iso}}$ ) parameter is almost independent of the direction of the external magnetic field while this dependency is available for anisotropic CS [17]. Quantum chemical calculations yield the CS eigenvalues in principal axes system (PAS) ( $\sigma_{33} > \sigma_{22} > \sigma_{11}$ ); therefore, (1) and (2) are used to convert them into the  $\sigma_{\text{iso}}$  and

Table 2. CS parameters of the (4,4) BP-NT.<sup>a</sup>

Atoms	$\sigma_{\text{iso}}$ (ppm)	$\Delta\sigma$ (ppm)	Atoms	$\sigma_{\text{iso}}$ (ppm)	$\Delta\sigma$ (ppm)
B1	36	136	P1	416	142
B2	35	122	P2	360	246
B3	40	109	P3	356	244
B4	43	112	P4	359	245
Average values of B for NT	38	120	Average values of P for NT	373	219
Average values of B for layer-like structure	61	127	Average values of P for layer-like structure	383	290

<sup>a</sup> See Fig. 1a for the atomic numbers.

Table 3. CS parameters of the (6,0) BP-NT.<sup>a</sup>

Atoms	$\sigma_{\text{iso}}$ (ppm)	$\Delta\sigma$ (ppm)	Atoms	$\sigma_{\text{iso}}$ (ppm)	$\Delta\sigma$ (ppm)
B1	40	126	P1	334	276
B2	25	118	P2	342	248
B3	31	116	P3	374	249
B4	18	144	P4	382	117
Average values of B for NT	28	126	Average values of P for NT	358	222
Average values of B for layer-like structure	49	131	Average values of P for layer-like structure	362	228

<sup>a</sup> See Fig. 1c for the atomic numbers.

$\Delta\sigma$  parameters, respectively (Tables 2 and 3).

$$\sigma_{\text{iso}} \text{ (ppm)} = \frac{1}{3}(\sigma_{11} + \sigma_{22} + \sigma_{33}), \quad (1)$$

$$\Delta\sigma \text{ (ppm)} = \sigma_{33} - \frac{1}{2}(\sigma_{11} + \sigma_{22}). \quad (2)$$

### 3. Results and Discussion

#### 3.1. Structures

The structures of the (4,4) and (6,0) BP-NTs (Fig. 1) and also the equivalent layer-like structures are optimized and the B-P average bond lengths, band gap energies, stabilization energies, and binding energies are presented in Table 1. It is noted that the layer-like structures include two structures with the number of atoms according to the number of atoms of the (4,4) and (6,0) NTs, separately. The calculations are also done on the layer-like structures to compare their results with those of the NTs. The average B-P bond length of 1.89 Å and 1.90 Å are, respectively, observed for the optimized (4,4) and (6,0) BP-NTs while these lengths are some shorter in the layer-like structures. The calculated B-P bond lengths are almost in agreement with that of the bulk BP with the length of 1.94 Å [15]. In comparison with the BN-NTs with average binary B-N bond length of 1.45 Å, there are longer binary bonds in the BP-NTs. However, parallel to the BN-NTs structure which N atoms orient outward and B atoms orient inward of the nanotube wall, the P atoms are oriented outward and the B atoms are oriented inward the wall

of the BP-NTs. The diameter of the armchair model in the end and middle of the nanotube are 7.85 Å and 6.92 Å, respectively, meaning that the ends of the nanotube are wider than the middle part. The diameter of the zigzag model in the B-end and P-end of the nanotube are 5.85 Å and 6.65 Å, respectively, meaning that the P-end is wider than the B-end. Due to more numbers of electrons in the valence shell of P rather than those of B, this trend is reasonable. In the corresponding layer like structures, which have two different types of zigzag and armchair ends, one type of ends has been saturated by the H atoms whereas the other type of ends has been left unsaturated. For the corresponding layer-like structure of the armchair model, the armchair ends have been saturated by the H atoms whereas the zigzag ends have been left unsaturated (Fig. 2a). For the corresponding layer-like structure of the zigzag model, the zigzag ends have been saturated by the H atoms whereas the armchair ends have been left unsaturated (Fig. 2b). The calculated stabilization energies of the investigated finite NTs and layer-like structures show that the NTs structures could be more stable than the layer-like structures in both of the (4,4) and (6,0) models. Furthermore, the binding energy, which is defined here to be the energy difference between the investigated finite NT and the corresponding layer-like structure, of the (4,4) model is smaller than that of the (6,0) model which means that formation of armchair BN-NT is more favorable rather than that of the zigzag model. Certainly, the binding energy is defined to be the energy difference between the infinite NTs and the corresponding infinite layer-

like structures; however, with the Gaussian 98 package, the finite structures could only be dealt with in present study. The band gap energies show that the BP-NTs and the layer-like structures are almost semiconductors but this property is much more observed in the NTs. It is also noted that the band gap energy of the armchair NT is some larger than that of the zigzag one. The reported experimental band gap energy for BP is 2.10 eV [27], however, previous DFT study yielded the values of 1.18, 1.24, and 1.86 eV [6] based on using different methods of calculations.

### 3.2. Chemical Shielding Parameters of the (4,4) BP-NT

The CS parameters of the optimized (4,4) BP-NT (Fig. 1a) and the average values for the equivalent layer-like structure are presented in Table 2. The results reveal that the parameters of this nanotube are divided into some layers with similar electronic properties at each layer. By the considered armchair model of BP-NT, there are four sets of the CS parameters for each of the  $^{11}\text{B}$  and  $^{31}\text{P}$  nuclei.  $\sigma_{\text{iso}}$  is the average of the CS tensors while in  $\Delta\sigma$  the CS tensor in  $z$ -axis plays the major role. More orientation of the CS tensors in the  $z$ -axis for a nucleus reveals that the atom is more proper for interactions with external agents. For  $^{11}\text{B}$  nuclei, the values of  $\sigma_{\text{iso}}$  are increased from the end to the middle of the nanotube; however, the values of  $\Delta\sigma$  are decreased in the same direction. For  $^{31}\text{P}$  nuclei, the values of  $\sigma_{\text{iso}}$  are decreased from the end to the middle of the nanotube; however, the values of  $\Delta\sigma$  are increased in the same direction. These results indicate that boron atoms play the major role in the ends of BP-NTs for interactions with the external agents. It is also well known that the B atom is more electronegative than the P atom; therefore, this major role of B is expected. Previously, it was also shown that boron atoms in the end of the nanotube play the major role in determining the characteristic properties of BN-NTs. Comparing the average values of NT with those of the layer-like structure reveals that for both, B and P, the CS parameters are larger in the latter structure.

### 3.3. Chemical Shielding Parameters of the (6,0) BP-NT

The CS parameters of the optimized (6,0) BP-NT (Fig. 1c) and the average values for the equivalent layer-like structure are presented in Table 3. In comparison with the armchair BP-NT, there are two differ-

ent ends, B-end and P-end, in the zigzag BP-NT; therefore, some different results are expected for this structure. B1 is the B-end and P4 is the P-end of the considered zigzag BP-NT. The CS parameters are divided into four layers for each of the  $^{11}\text{B}$  and  $^{31}\text{P}$  nuclei. In this structure, B1 has the largest values of  $\sigma_{\text{iso}}$  and  $\Delta\sigma$  among other B-layers. By going to the opposite side of the nanotube, the P-end, the magnitudes of these parameters are reduced, where B4 placed in the nearest neighbourhood of P-end has the smallest value of  $\sigma_{\text{iso}}$ . However, it seems that placing in the nearest neighbourhood of P-end, the CS tensors of B4 orient into the  $z$ -axis yielding the largest value of  $\sigma_{\text{iso}}$  among other B-layers. For P-layers, P4 has the largest value of  $\sigma_{\text{iso}}$  but the smallest value of  $\Delta\sigma$  through other P-layers. The harmonic changes of these parameters from P-end to B-end are observed here with  $\sigma_{\text{iso}}$  decrease while  $\Delta\sigma$  increase from P4 to P1. This trend is in agreement with that of the armchair model; however, some discrepancies are observed for the  $\Delta\sigma$  results of B-layers. As mentioned earlier, the electronic structures of zigzag and armchair BP-NTs are different; therefore, some exceptions are expected in their results. In this case, the exception is viewed just for B4 in the zigzag model which instead of having the smallest  $\Delta\sigma$  value has the largest one. It is noted that parallel to the results of armchair model, this value is decreased from B1 to B3 but it is unexpectedly increased just for B4. Comparing the average CS values of the layer-like and the NT structures show that the layer-like structure still has the larger values; this trend is in agreement with the results of the armchair model.

## 4. Conclusions

The structure properties of the (4,4) and (6,0) BP-NTs are studied by DFT calculations of the energies and the CS parameters in the optimized structures of NTs and layer-like models. The comparison of the stabilization energies shows that the NTs models are more stable than the layer-like ones. Furthermore, the band gap energies are also increased in the NTs models regarding to the layer-like structures. The CS parameters are divided into some layers with equivalent electronic properties. In the armchair model, from the end to the middle of the nanotube, the  $\sigma_{\text{iso}}$  values of  $^{11}\text{B}$  are increased while those of  $^{31}\text{P}$  are decreased. In contrast, the  $\Delta\sigma$  values of  $^{11}\text{B}$  are decreased while those of  $^{31}\text{P}$  are increased in the same direction. In the zigzag model, from P-end to B-end, parallel results are ob-

served for  $^{31}\text{P}$  while discrepancies for  $^{11}\text{B}$  results. The major difference in the results is that the  $\Delta\sigma$  value of  $^{11}\text{B}$  for B4 is the largest although it is in the nearest neighbourhood of the P-end.

- [1] S. Iijima, *Nature* **354**, 2148 (1991).
- [2] Ş. Erkoç and H. Kökten, *Physica E* **28**, 162 (2005).
- [3] A. Loiseau, F. Willaime, N. Demoncey, N. Schramcheko, G. Hug, C. Colliex, and H. Pascard, *Carbon* **36**, 743 (1998).
- [4] N. G. Chopra, R. J. Luyken, K. Cherrey, V. H. Crespi, M. L. Cohen, S. G. Louie, and A. Zettl, *Science* **269**, 966 (1995).
- [5] A. Rubio, J. L. Corkill, and M. L. Cohen, *Phys. Rev. B* **49**, 5081 (1994).
- [6] R. Ahmed, Fazal-e-Aleem, S. J. Hashemifar, and H. Akbarzadeh, *Physica B* **403**, 1876 (2008).
- [7] S. Hou, Z. Shen, J. Zhang, X. Zhao, and Z. Xue, *Chem. Phys. Lett.* **393**, 179 (2004).
- [8] D. Zhang and R. Q. Zhang, *Chem. Phys. Lett.* **371**, 426 (2003).
- [9] S. C. Jain, M. Willander, J. Narayanan, and R. van Overstraeten, *J. Appl. Phys.* **87**, 965 (2000).
- [10] Z. Bagheri, M. Mirzaei, N. L. Hadipour, and M. R. Abolhassani, *J. Comput. Theor. Nanosci.* **5**, 614 (2008).
- [11] M. Zhao, Y. Xia, Z. Tan, X. Liu, F. Li, B. Huang, Y. Ji, D. Zhang, and L. Mei, *Chem. Phys. Lett.* **389**, 160 (2004).
- [12] Ş. Erkoç, O. B. Malciolu, and E. Taşci, *J. Molec. Struct. (Theochem)* **674**, 1 (2004).
- [13] Z. Qian, S. Hou, J. Zhang, R. Li, Z. Shen, X. Zhao, and Z. Xue, *Physica E* **30**, 81 (2005).
- [14] Ş. Erkoç, *J. Molec. Struct. (Theochem)* **676**, 109 (2004).
- [15] V. A. Ferreira and H. W. Leite Alves, *J. Cryst. Growth* **310**, 3973 (2008).
- [16] E. Schrotten, A. Geossens, and J. Schoonman, *J. Appl. Phys.* **83**, 1660 (1998).
- [17] F. A. Bovey, *Nuclear Magnetic Resonance Spectroscopy*, Academic Press, San Diego 1988.
- [18] M. Mirzaei, *Physica E* **41**, 883 (2009).
- [19] M. Mirzaei, *Z. Phys. Chem.* **223**, 815 (2009).
- [20] M. Mirzaei, A. Seif, and N. L. Hadipour, *Chem. Phys. Lett.* **461**, 246 (2008).
- [21] M. J. Frisch, G. W. Trucks, H. B. Schlegel, G. E. Scuseria, M. A. Robb, J. R. Cheeseman, V. G. Zakrzewski, J. A. Montgomery, Jr., R. E. Stratmann, J. C. Burant, S. Dapprich, J. M. Millam, A. D. Daniels, K. N. Kudin, M. C. Strain, O. Farkas, J. Tomasi, V. Barone, M. Cossi, R. Cammi, B. Mennucci, C. Pomelli, C. Adamo, S. Clifford, J. Ochterski, G. A. Petersson, P. Y. Ayala, Q. Cui, K. Morokuma, D. K. Malick, A. D. Rabuck, K. Raghavachari, J. B. Foresman, J. Cioslowski, J. V. Ortiz, A. G. Baboul, B. B. Stefanov, G. Liu, A. Liashenko, P. Piskorz, I. Komaromi, R. Gomperts, R. L. Martin, D. J. Fox, T. Keith, M. A. Al-Laham, C. Y. Peng, A. Nanayakkara, C. Gonzalez, M. Challacombe, P. M. W. Gill, B. Johnson, W. Chen, M. W. Wong, J. L. Andres, C. Gonzalez, M. Head-Gordon, E. S. Replogle, and J. A. Pople, *Gaussian 98*, Gaussian, Inc., Pittsburgh, PA, 1998.
- [22] K. Wolinski, J. F. Hinton, and P. Pulay, *J. Am. Chem. Soc.* **112**, 8251 (1990).
- [23] F. J. London, *Phys. Radium* **8**, 397 (1937).
- [24] R. Ditchfield, *Mol. Phys.* **27**, 789 (1974).
- [25] F. Ribas Prado, C. Giessner-Prettre, J.-P. Daudey, A. Pullman, F. Young, J. F. Hinton, and D. J. Harpool, *Magn. Reson.* **37**, 431 (1980).
- [26] H. Fukui, K. Miura, H. Yamazaki, and T. Nosaka, *J. Chem. Phys.* **82**, 1410 (1985).
- [27] R. W. G. Wyckoff, *Crystal Structures*, second ed., Krieger, Malabar 1986.